Spatial Heterogeneity in a Polymer Thin Film Probed by Single Molecules

Vasudevan Pillai Biju,*,† Jing Yong Ye,‡ and Mitsuru Ishikawa*

Single Molecule Bioanalysis Laboratory, National Institute of Advanced Industrial Science and Technology (AIST, Shikoku), 2217-14 Hayashi-cho, Takamatsu, Kagawa 761-0395, Japan

Received: April 9, 2003; In Final Form: July 13, 2003

Spatial heterogeneity in a polymer melt has been divided into two distributions that are distinguished by different relaxation behaviors of single-molecule probes near the nominal calorimetric glass-transition temperature (T_g). The fluorescence intensity and lifetime of individual molecules in a polymer film each exhibited a bimodal histogram that involved fast- and slow-relaxation sites at $T_g - 8$ K and $T_g + 7$ K, whereas a monomodal histogram composed of fast-relaxation sites was observed at $T_g + 30$ K. Temperature has no important effect on the center of each distribution in these histograms. Instead, occurrences of slow-relaxation sites decreased as the temperature increased from $T_g - 8$ K to $T_g + 7$ K and disappeared at $T_g + 30$ K. Furthermore, a change in the single-molecule fluorescence intensity was traced at fast- and slow-relaxation sites in a polymer film. At $T_g - 8$ K and $T_g + 30$ K, no substantial change in fluorescence intensity was observed at each site for ≥ 3 h, whereas, at $T_g + 7$ K, the fluorescence intensity varied with an average time constant of 200−300 s at fast- and slow-relaxation sites. This variation comes most likely from a cooperative rearrangement of fast- and slow-relaxation sites, not from a migration of the single molecules between static fast- and slow-relaxation sites.

Introduction

People have known how to make glassy objects since ancient times; however, the physics underlying glass transition remains an unsolved central issue in condensed matter science, even today. The origin of glass transition has been determined to be dynamical events rather than phase transitions.[1] Thus, many studies have focused on the dynamics of glass transition.[2−8] Nonexponential relaxation was observed in various liquids and polymers near the glass-transition temperature (T_g). This nonexponential feature was attributed to dynamic heterogeneity within the framework of mode-coupling theory (MCT).[9,10] Also, experimental studies[11,12] supported the idea of dynamic heterogeneity; however, these studies neglected spatial heterogeneity. On the other hand, many attempts have been made to address the spatial heterogeneity.[13−16] However, the discussion was inevitably not straightforward, because the nanoscale heterogeneity is masked by spatially averaging over different sites in conventional ensemble measurement.

A single-molecule approach to the issue of glass transition could provide an ultimate solution to disclose every minute detail of the mystery underlying this issue. In recent single-molecule studies,[17,18] the dynamics in polymer films was investigated by tracing the rotational motion of a single molecule in real time using confocal microscopy. These studies elucidated nonexponential rotational relaxation of individual molecules and site-dependent broad distribution of the relaxation time, which showed a dependence on the length of observation time. Our approach, on the other hand, is different from the previous single-molecule studies in three ways. First, we observed the fluorescence intensity and lifetime of single molecules, not rotational motion, to evaluate the site-sensitive dynamics. This approach is motivated by our previous study that was based on fluorescence lifetime measurement of a viscosity-sensitive dye molecule.[16] Second, we used single molecules that were covalently immobilized on a glass surface and overlaid with a polymer film. Last, we used wide-field microscopy. This approach is advantageous for the simultaneous evaluation of the spatial distribution of many single molecules, thereby allowing the quantitative construction of histograms of the fluorescence intensity of many single molecules.

Experimental Section

Sample Preparations. Fundamental properties of the single-molecule samples prepared by the covalent bonding technique are described in the work by Biju et al.[19] The chemical procedures that they used are described again here. First, an aminosilanized glass surface was prepared by dipping a slide glass in an ethanolic solution (1 μM) of 3-aminopropyltrimethoxy silane (AZmax, Tokyo) for 30 min at 22 °C. Excess reagent was washed out repeatedly (five times each) with ethanol (Wako, Tokyo) and water before the glass surface was incubated at 50 °C for 1 h. A Na_2CO_3:$NaHCO_3$ (Wako, Tokyo) buffer solution (pH 9.8) of a succinimide derivative of Cy3 dye (2 nM; Molecular Probes, Eugene, OR) then was allowed to react with one side of the aminosilanized glass surface for 30 min at 22 °C in darkness. Excess dye molecules were washed out repeatedly (five times each) with water and ethanol, and the surface was dried using a jet of nitrogen gas. Finally, Cy3 molecules that had been immobilized on a glass surface were overlaid with a poly(vinyl acetate) (PVAc, average molecular mass of 167 000; Aldrich, Tokyo) film by spin coating a PVAc solution (100 μM) in ethyl acetate (Wako, Tokyo) at 3000 rpm. The thickness of the polymer film was determined to be ~100 nm, using a stylus profiler (DEKTAK^{3}ST, Veeco, Santa Barbara,

* Authors to whom correspondence should be addressed. E-mail: ishikawa-mitsuru@aist.go.jp, vasudevan.pillai.biju@pnl.gov.

† Current address: Chemical Structure and Dynamics Group, Pacific Northwest National Laboratory, Richland, WA 99352.

‡ Current address: Center for Ultrafast Optical Science, University of Michigan, 2200 Bonisteel Blvd., Ann Arbor, MI 48109.

10.1021/jp034942c CCC: $25.00
Published on Web 09/06/2003

CA). The sample was dried in air overnight to remove the solvent. Spin coating a polymer overlayer on single molecules on a glass surface enables the single molecules to be in a polymer environment.[20] Also, spin-coated thin polymer films have been identified as good candidates to study polymer dynamics near interfaces.[21−24]

Covalent bonding highly ensures single molecules to be isolated on a glass surface compared with spin coating.[19] There are three advantages of the covalent bonding over spin coating. First, dye molecules in our sample are free from an interface effect between a polymer layer and air if a polymer layer on single molecules has sufficient thickness (>10 nm or more). Second, excess dye molecules on a sample surface are washable, to be helpful in getting single molecules well isolated on a glass surface. Last, single molecules on a glass surface are free from migration, even after a polymer layer is spin-coated. The immobilization makes it possible to compare a surface before and after spin-coating a polymer layer. For these reasons, we prefer covalent bonding to spin coating. Despite this preference, spin coating was used to eliminate the possibility that an artifact from an interface between a glass surface and a PVAc film, as well as interaction of dye molecules with glass surface, is dominant in the fluorescence intensity and lifetime measurements. We tested two methods other than covalent bonding. One method is the use of a mixture of Cy3 (2 nM) and PVAc (100 μM) in ethyl acetate (100 μL) for spin coating on a glass surface at 3000 rpm; the other method is the sandwiching of Cy3 molecules between two PVAc films. For the latter procedure, a PVAc solution (50 μL, 100 μM) in ethyl acetate was spin-coated on a glass surface at 3000 rpm, followed by the spin coating of a Cy3 solution (100 μL, 2 nM) in methanol, finally covering the Cy3 molecules by spin coating a PVAc solution (50 μL, 100 μM) in ethyl acetate. Photobleaching kinetics was observed to identify the number of Cy3 molecules included in each fluorescent spot. Single fluorescent spots selected at random always exhibited staircase photobleaching in a single step, thus verifying that each site contains only a single molecule in samples that have been prepared by covalent bonding. The histograms of fluorescence photocounts and lifetimes were independent of the methods used to prepare samples, except for the contribution of grouping of single Cy3 molecules in samples that had been prepared using spin coating.[25]

Instruments Used. The fluorescence images and lifetimes of single Cy3 molecules were obtained using wide-field video microscopy plus time-resolved fluorometry.[19,25−28] The use of wide-field microscopy in the current method enabled us to evaluate the spatial distribution of many single molecules simultaneously and to obtain histograms of the fluorescence intensity of many single molecules quantitatively. The temperature was controlled using a temperature controller (model ITC503, Oxford Instruments, Tokyo) for imaging and lifetime experiments.

Quantitative evaluation of the histograms of fluorescence photocounts of single molecules is essential to the current study. Thus, we utilized the following two key techniques. One technique is the use of a continuous wave (cw) circularly polarized light (532 nm) for unbiased excitation of single molecules,[29] and the other technique is the use of a single-photon counting (SPC) video camera. Without the SPC technique, the distribution of photocounts is modified by detector-generated and post-detector electronic noise of the video camera.[19] However, to trace the trajectories of single-molecule fluorescence intensity in real time, we used a charge-coupled device (CCD) camera that was equipped with a highly efficient image intensifier[19,25] in place of a SPC video camera.

For fluorescence lifetime measurements, 150-fs pulses generated from a Coherent model OPA 9400 optical parametric amplifier (OPA) was tuned to 540 nm at a repetition frequency of 200 kHz. This OPA was pumped with a regenerative amplifier (Coherent, model RegA 9000) seeded from a mode-locked Ti:sapphire laser (Coherent, model Mira 900F). The 540-nm pulses were used as the excitation source for single Cy3 molecules. The fluorescence lifetime of individual molecules was measured in the following manner. The fluorescence image of a single molecule was selected among many single-molecule fluorescence images, using a video microscope system. This system was composed of an optical microscope (model Axioplan, Zeiss) and a CCD camera that was equipped with a highly efficient image intensifier. The selected fluorescence image of a single molecule was filtered through a pinhole placed on the image plane of the optical microscope. The filtered fluorescence was focused on the entrance slit of a polychromator (Chromex, model 250IS) that was coupled with a photon-counting streak scope (Hamamatsu, model C4334).[26]

Results and Discussion

We selected Cy3 dye as a site-sensitive probe (see the molecular structure in Figure 1A) and PVAc (see the molecular structure in Figure 1B) as a representative polymer, whose T_g (30 °C) is close to room temperature (22 °C). Restriction of segmental motion is the key factor of the environment-sensitive fluorescence efficiency and lifetime of Cy3.[30−35] Thus, the dimensions involved in our approach are different from those involved in the rotational motion of dye molecules in a polymer film.[17,18] We characterized the environment sensitivity of the fluorescence properties of Cy3 by examining the fluorescence efficiency and lifetime of bulk solutions of Cy3 in water−glycerol mixtures, as well as in the presence of α-, β-, and γ-cyclodextrins (CDs). The fluorescence efficiency of Cy3 dye showed a sixfold enhancement in glycerol, compared to that in water, and its fluorescence lifetime increased from 0.22 ns in water to 2.02 ns in glycerol. Also, the addition of a β-CD solution to an aqueous solution of Cy3 resulted in a 1.3-fold enhancement in the fluorescence efficiency, and the fluorescence lifetime increased from 0.22 ns in water to 0.89 ns in the presence of 30 mM β-CD. The increase in fluorescence efficiency and lifetime of Cy3 dye in the presence of glycerol or CD is attributed to restriction of conformational motion of dye molecules, thereby reducing the rate of nonradiative decay of the lowest excited singlet state in constrained environments (for details, see Supporting Information, which is available online).

Isolated fluorescent spots of single Cy3 molecules covalently immobilized on a glass surface were observed without (Figure 1C) and with (Figure 1D) a 100-nm-thick PVAc overlayer at 22 °C (T_g − 8 K). The upper and lower traces in Figure 1E compare the intensity profile in an area in Figure 1C and that in Figure 1D, respectively. Note that variation in the fluorescence intensity is enhanced with a PVAc overlayer. A monomodal histogram of fluorescence photocounts of individual spots was found without a PVAc overlayer (Figure 2A), whereas a bimodal histogram was observed with a PVAc overlayer (Figure 2B). From these two observations, we consider that the bimodality is not intrinsic to Cy3 but is due to interaction between Cy3 and a PVAc overlayer. Moreover, the possibility of any interface effect on the bimodality, such as two types of Cy3 molecules, stuck on a glass surface and embedded in a

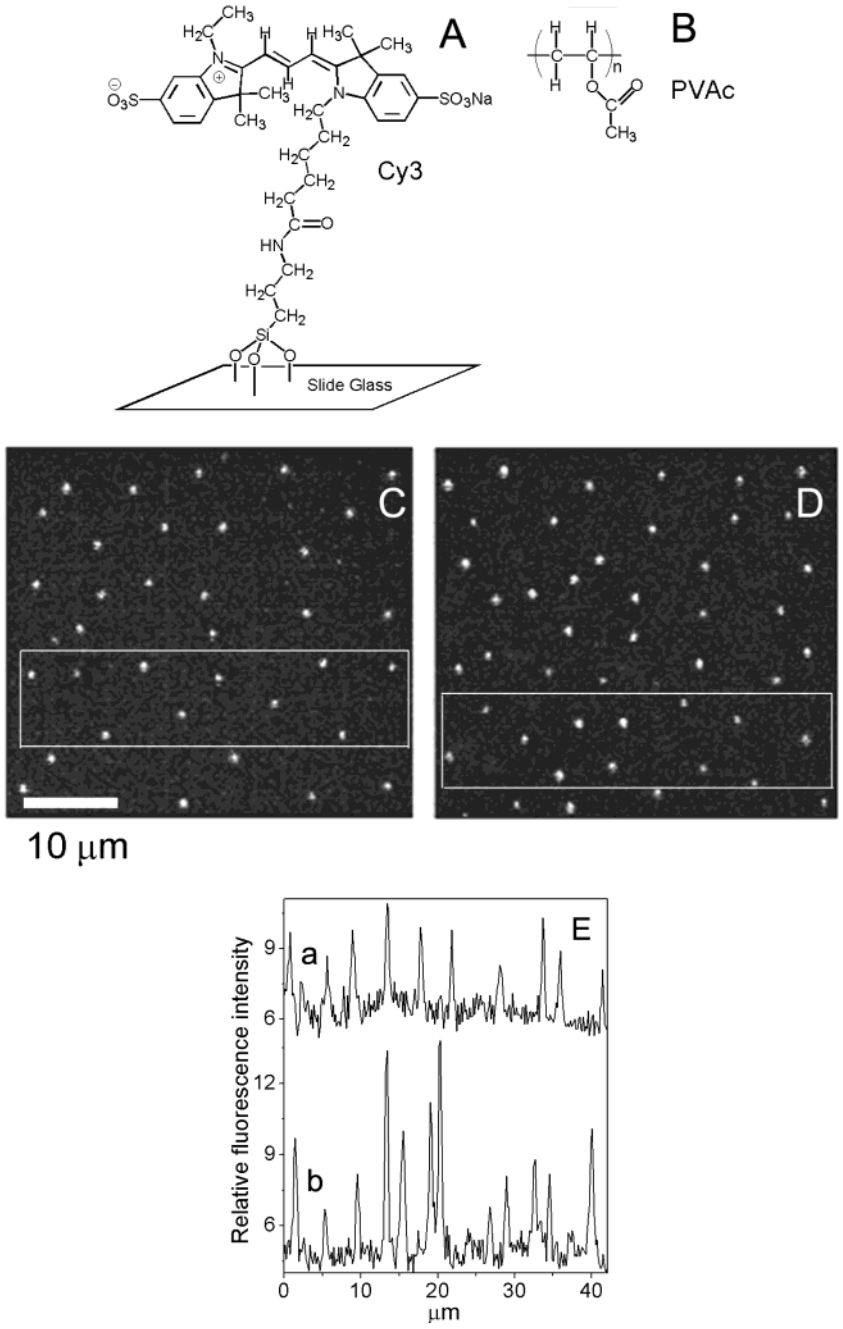

Figure 1. (A) Molecular structure of Cy3 covalently immobilized on a glass surface. (B) Molecular structure of PVAc. (C) Fluorescence image of single Cy3 molecules covalently immobilized on a glass surface without a poly(vinyl acetate) (PVAc) overlayer. (D) Fluorescence image of single Cy3 molecules covalently immobilized on a glass surface with a PVAc overlayer. Images in panels C and D both were recorded for 1 min at 22 °C, using a far-field light microscope that was equipped with a single-photon-counting (SPC) video camera. A continuous wave (cw) circularly polarized 532-nm laser (providing 12 mW of power (1 W/cm^2)) was used for excitation. (E) Intensity profiles for single Cy3 molecules; the upper trace (trace a) represents the intensity profile of an area clipped from the image shown in panel C, and the lower trace (trace b) represents that from the image shown in panel D. Note that the intensity variations in trace b are larger than those in trace a, because of the presence of a PVAc overlayer.

PVAc overlayer, has been excluded from retention of bimodality, irrespective of whether a sample is prepared by (i) the covalent bonding of dye molecules, followed by the spin coating of a PVAc film, (ii) the sandwiching of Cy3 molecules between two PVAc films, or (iii) the spin coating of a mixed PVAc−Cy3 solution. Also, the possible contribution of low-intensity fluorescence spots that result from the photobeaching of dye molecules within the time under image acquisition (1 min in our case) to the occurrences of molecules with low steady-state intensity is negligible, according to the photochemical stability of Cy3 molecules for several hundreds of seconds in a polymer film under the current experimental conditions. We thus conclude that the bimodal histogram reflects the fundamental nature of Cy3 molecules that are embedded in PVAc.

Under unbiased excitation using circularly polarized light, we have two cases that make the histogram of fluorescence intensity bimodal. One case is a difference in absorbance in resonance with 532-nm excitation. The other case is a difference in fluorescence efficiency, or lifetime. Fluorescence lifetimes of individual Cy3 molecules that have been covalently immobilized on a glass surface and overlaid with a PVAc film were measured at a temperature of $T_g - 8$ K to determine which

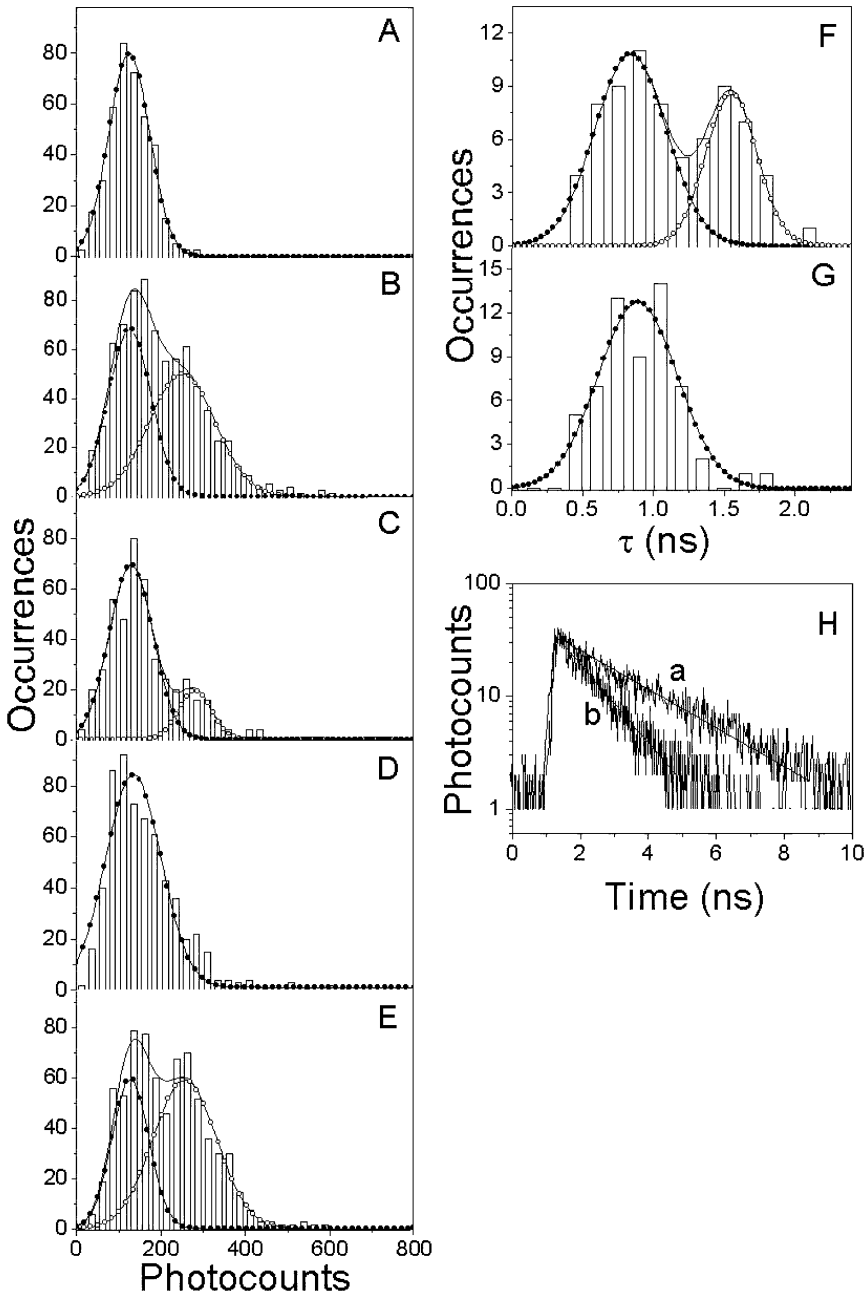

Figure 2. Histograms of fluorescence photocounts from single Cy3 molecules covalently immobilized on a glass surface: (A) without a PVAc overlayer, at $T_g - 8$ K; (B) overlaid with a PVAc film, at $T_g - 8$ K; (C) overlaid with a PVAc film, at $T_g + 7$ K; (D) overlaid with a PVAc film, at $T_g + 30$ K; and (E) overlaid with a PVAc film, at $T_g - 8$ K after repeatedly heating and cooling between $T_g + 30$ K and $T_g - 8$ K. Panels F and G show histograms of fluorescence lifetimes of single Cy3 molecules covalently immobilized on a glass surface and overlaid with a PVAc film at $T_g - 8$ K (panel F) and $T_g + 30$ K (panel G). The ball-joint lines represent Gaussian fits and are used to compare the area of each Gaussian distribution. Panel H shows fluorescence decay curves of a representative single Cy3 molecule covalently immobilized on a glass surface overlaid with a PVAc film at $T_g - 8$ K ($\tau_f = 1.73$ ns, trace a) and $T_g + 30$ K ($\tau_f = 0.88$ ns, trace b).

case is important for a difference in the fluorescence intensity. Figure 2F shows that a bimodal distribution occurred in the histogram of fluorescence lifetimes. This histogram includes two distributions that are centered at 0.89 and 1.60 ns and is consistent with the photocount counterpart. This lifetime histogram reveals that, in a bimodal histogram, the low-intensity distribution is ascribed to fast-relaxation sites, which are equivalent to a low viscosity of the surrounding PVAc, whereas the high-intensity distribution comes from slow-relaxation sites, which are equivalent to a higher viscosity of the surrounding PVAc.

Bimodal distribution does not mean that two definite sites are included in the distribution. We have narrowly succeeded in dividing a wide distribution of inhomogeneous sites into two classes with the help of single-molecule fluorescence measurement. Experimental observation of bimodal distribution suggests that nonexponential relaxation in glass-forming materials is not always well described using a single stretched exponential function. Indeed, a recent study concluded that it is necessary to use a function that includes two stretched exponential terms to describe the relaxation processes in the glass transition of PVAc.[36] More recently, a theoretical study foresaw the bimodal nature in a supercooled liquid.[37] In addition to our previous studies that have addressed bimodal heterogeneity,[16,28,38] our current observations could stimulate theoretical studies of the bimodal heterogeneity of liquids and polymers near the T_g value.

The temperature dependence of a bimodal histogram was investigated to determine the change that occurs in the bimodal distribution. For this purpose, histograms of fluorescence photocounts and lifetimes were constructed again at temperatures greater than $T_g - 8$ K, using the same sample. A bimodal nature was observed again at $T_g + 7$ K in the histogram of fluorescence photocounts (see Figure 2C). The ratio of fast-relaxation sites to slow-relaxation sites is 1:1.1 at $T_g - 8$ K and 1:0.21 at $T_g + 7$ K. Thus, the contribution of slow-relaxation sites to the histogram decreased as the temperature increased. Moreover, at $T_g + 30$ K, the occurrences of slow-relaxation sites disappeared in the photocount histogram (see Figure 2D) and also in the lifetime histogram (see Figure 2G). These observations are ascribed to a change in local environments around single Cy3 molecules in a PVAc film, rather than a direct temperature effect on Cy3 fluorescence. If a direct temperature effect on Cy3 is important, a change in distribution from bimodal to monomodal should be observed without host matrixes. However, the monomodal distribution (Figure 2A) without a PVAc overlayer remained unchanged during elevation of the temperature from 22 °C to 60 °C. Furthermore, the use of poly(methyl methacrylate) (PMMA, $T_g = 114$ °C) strongly demonstrated the importance of the T_g value of host matrixes. The histogram was always bimodal in the range of 22−60 °C for single Cy3 molecules that have been covalently immobilized on a glass surface and overlaid with a PMMA film (data not shown). Also, the possibility that a change in the histogram from bimodal to monomodal may be due to evaporation of the solvent (ethyl acetate) used in preparing a PVAc solution was eliminated. This elimination was based on the reconstruction of the histogram after cooling the same sample back from $T_g + 30$ K to $T_g - 8$ K. The histogram changed back from monomodal to bimodal (see Figure 2E). The bimodal nature in the histogram was retained, even after 10 or more heating-and-cooling cycles between $T_g - 8$ K and $T_g + 30$ K, although the maximums of the histograms and the ratio of the slow- to fast-relaxation sites did not provide exactly the same values on each occasion. The slight variations in these parameters are understandable, because it is widely known that the glass formation is dependent on the cooling history.

Summarizing the temperature effect on the histograms, temperature has no important effect on the center of fast- and slow-distribution in each histogram. Instead, occurrences of slow-relaxation sites decreased as the temperature increased from $T_g - 8$ K to $T_g + 7$ K and disappeared at $T_g + 30$ K, without changing the center of each distribution. This disclosure is favored by our single-molecule measurements. In conventional ensemble measurements, only the overall change in the fluorescence intensity and lifetimes is observed as the temperature changes. Variation in the distributions of fluorescence photocounts and lifetimes in the histograms, as a function of temperature, further exclude the possibility that an interface effect contributes to the bimodal nature of photocount and lifetime histograms due to two types of dye molecules (one type is stuck on the glass surface, and the other type is embedded in the polymer film). Here, remember that cyanine dye molecules in a viscous environment are widely known to have enhanced fluorescence efficiency. The ratio of the number of molecules stuck on a glass surface to those embedded in a polymer film, if such an effect is important, is expected to decrease as the temperature increases, because of the increase in the thermal energy of the molecules. Therefore, if an interface effect is important in our observation, contributions of the molecules embedded in a polymer film should reflect enhancements in the long lifetime and high fluorescence intensity components in the corresponding histograms as the temperature is increased from 22 °C to 60 °C, or vice versa as the temperature is decreased. However, this inference is not the case. Our current observations showed an increase in the contribution of short-lifetime and low-intensity components to the histograms with increasing temperature and vice versa with decreasing temperature. These observations clearly indicate that the interface-induced difference in the orientation of dye molecules is not the major factor, if not completely eliminated, in regard to being responsible for the bimodal and monomodal nature of the lifetime and photocount histograms.

We are now ready to focus on each site that constitutes a histogram near the T_g value. Figure 2H shows fluorescence decay curves of a single Cy3 molecule in a slow-relaxation site at temperatures of $T_g - 8$ K and $T_g + 30$ K, respectively. The lifetime was 1.73 ns at $T_g - 8$ K (trace a in Figure 2H) and 0.88 ns at $T_g + 30$ K (trace b in Figure 2H). In a fast-relaxation site, only a minor effect of temperature on the lifetime was observed, within the limits of experimental errors: 0.94 ns at $T_g - 8$ K and 0.98 ns at $T_g + 30$ K. The variable lifetime at a slow-relaxation site and the invariable lifetime at a fast-relaxation site are consistent with the histograms in Figure 2F and G.

Evaluation of the variable or invariable nature of each site by lifetime measurement suffers the technical drawback of requiring a long period of time (>300 s in our experiments). Conveniently enough, we have already observed that a change in fluorescence intensity is dominated by a change in the fluorescence lifetime. Thus, tracing a change in fluorescence intensity is an alternative way to follow a change in the dynamics in each site in real time. At $T_g - 8$ K and $T_g + 30$ K, no substantial change was observed in the fluorescence intensities of single molecules for ≥3 h. This constant nature will be precisely the reason for the observation of single-exponential fluorescence decays in Figure 2H. In contrast, we observed an intensity exchange among individual fluorescent spots at $T_g + 7$ K. Figure 3A and B show that, at $T_g + 7$ K, some spots changed from low intensity to high intensity (solid circles), some did the reverse (dotted circles), and the spots that remain (no circles) did not show any substantial variation in intensity, even after 1 h. Note that the images in Figure 3A and B were collected from the same field of view but at different times.

To collect more information on the variation in fluorescence intensity, especially at $T_g + 7$ K, we continuously recorded the trajectories of individual fluorescent spots for several hundreds of seconds. No variation was observed at $T_g - 8$ K and $T_g + 30$ K. On the other hand, some, but not all, trajectories showed up-and-down variations in the fluorescence intensity at $T_g + 7$ K. Figure 3C shows a high-intensity trajectory at $T_g - 8$ K (trace a), up-and-down trajectories at $T_g + 7$ K (traces b and c), and a trajectory at $T_g + 30$ K (trace d). Because Cy3 molecules are covalently immobilized on a glass surface, the migration of Cy3 chromophores is limited by the molecular tether that connects a Cy3 chromophore to a glass surface. Thus, the migration of a single Cy3 molecule among static heterogeneous environments over a possible dimension (∼1.4 nm) is excluded as being able to explain the up-and-down trajectories at $T_g + 7$ K. The radius of a hemisphere in which a Cy3 chromophore can move is limited by the length of the molecular tether that connects a Cy3 chromophore with a glass surface. The close contact distance (or effective distance),

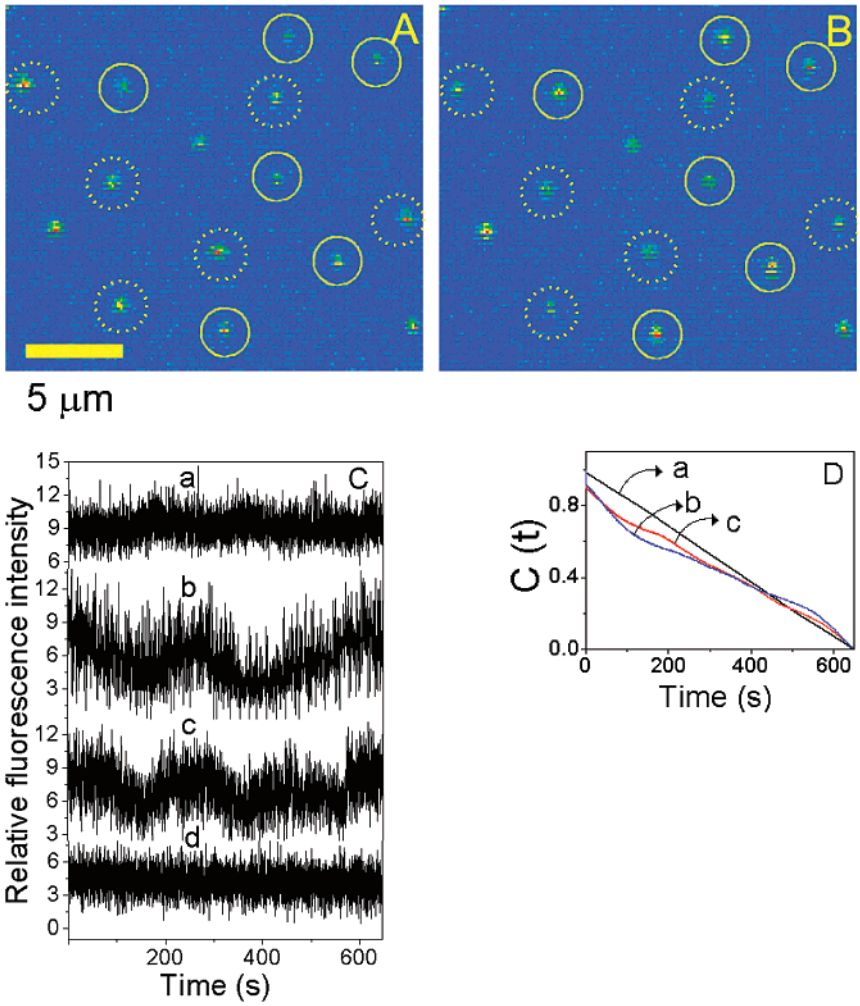

Figure 3. (A) Fluorescence image of single Cy3 molecules that have been covalently immobilized on a glass surface overlaid with a PVAc film at $T_g + 7$ K. (B) Fluorescence image of the same material as that in panel A, except this image was collected 1 h after the image in panel A was collected. Some spots show an increase in fluorescence intensity (solid circles), some spots show a decrease in fluorescence intensity (dotted circles), and the other spots (no circles) show no substantial change in fluorescence intensity. All the experimental conditions are the same as those in Figure 1. (C) Representative trajectories of fluorescence intensity of a single Cy3 molecule at $T_g - 8$ K (trace a), $T_g + 7$ K (traces b and c), and $T_g + 30$ K (trace d); a CCD camera equipped with a highly efficient image intensifier was used to record intensity trajectories in real time. (D) Autocorrelation functions of fluorescence intensity trajectories. Each autocorrelation function a, b, and c respectively corresponds to the trajectories a, b, and c in panel C. The autocorrelation of trajectory d (trace not shown) is similar to that of trajectory a. Autocorrelation of trajectory a appears a straight line, because trace a in panel C forms a rectangle wave by extending the range of time outside 0 to 660 s (e.g., from −200 s to 860 s). The autocorrelation of a rectangle waveform will show a straight line.

not the through-bond distance that joins each atom, of the molecular tether is 1.39 nm between a Si atom on a silanized glass surface and the N atom in Cy3 (see Figure 1A). In fact, this distance provides the upper limit of the radius. Actually, a possible range in which a Cy3 chromophore can move will be smaller than this distance. The possibility that the time evolution of the local PVAc structure that encloses a single-molecule probe causes the up-and-down trajectories is valid if the dimension of spatial heterogeneities is larger than the estimated dimension of ∼1.4 nm. Considering the predicted dimension of 1.53 nm (from Mohanty[13]) and the experimentally estimated value of 5 nm (from Achibat et al.[39]) by Raman scattering, we conclude that cooperative evolution of the local PVAc structure with time, rather than the migration of probe molecules, is important for the up-and-down trajectories.

The trajectories at the three temperatures clarify the requirement that, at $T_g + 7$ K, heterogeneous sites in a PVAc film evolve with time. Figure 3D shows the autocorrelation functions $C(t)$ of the trajectories in Figure 3C.

$$C(t) = \frac{\sum_{t'=0}^{T} I(t')I(t'+t)}{\sum_{t'=0}^{T} I(t')I(t')}$$

Here, $I(t)$ is the time-dependent fluorescence intensity and T is the total number of data points. From these autocorrelations, a persistent time of fast- and slow-relaxation sites was estimated to be ∼100−200 s. In contrast to the structural arrest at a critical temperature T_c higher than the T_g value predicted by the ideal MCT, our observation of the trajectory of fluorescence intensity in real time allows us to conclude that some sites evolve to new sites via large collective motions of PVAc that enclose a single Cy3 molecule at $T_g + 7$ K. Although the possibility for rearranging heterogeneous sites above T_g was predicted,[13] the current study provides substantial evidence that local rearrangement of individual sites occurred at $T_g + 7$ K. This disclosure is specific to the use of covalently immobilized single molecules

and the dimensions that are involved in the current approach of fluorescence intensity and lifetime measurements.

Conclusions

Current single-molecule fluorescence imaging and lifetime measurements provide an effective approach for mapping spatially heterogeneous sites in a polymer melt near the glass-transition temperature (T_g) and allow information about the ratio between fast- and slow-relaxation sites to be obtained. We observed bimodal histograms of slow- and fast-relaxation sites in a PVAc film, the temperature dependence of bimodal histograms, and the cooperative rearrangement of different sites from fast to slow and vice versa at a temperature of $T_g + 7$ K. In addition to the significance of our current work shedding light on the long-standing mystery of the physics underlying the glass transition, an understanding of the spatial heterogeneity is of practical importance to future single-molecule organic devices if these devices are embedded in glass-forming materials to support the structures. The temperature-dependent spatial heterogeneity in the supporting materials might strongly affect the functions and operation of these devices.

Supporting Information Available: Schematic presentation of covalent binding of Cy3 on a glass surface, bulk fluorescence properties of Cy3 in water−glycerol mixtures of varying composition, and effect of the presence of varying concentrations of α-, β-, and γ-cyclodextrins (PDF). These materials are available free of charge via the Internet at http://pubs.acs.org.

References and Notes

(1) Santen, L.; Krauth, W. *Nature* **2000**, *405*, 550−551.

(2) Bennemann, C.; Donati, C.; Baschnagel, J.; Glotzer, S. C. *Nature* **1999**, *399*, 246−249.

(3) Angell, C. A.; Ngai, K. L.; McKenna, G. B.; McMillan, P. F.; Martin, S. W. *J. Appl. Phys.* **2000**, *88*, 3113−3157.

(4) Wang, C.-Y.; Ediger, M. D. *J. Phys. Chem. B* **2000**, *104*, 1724−1728.

(5) Ediger, M. D. *Annu. Rev. Phys. Chem.* **2000**, *51*, 99−128.

(6) Weeks, E. R.; Crocker, J. L.; Levitt, A. C.; Schofield, A.; Weitz, D. A. *Science* **2000**, *287*, 627−629.

(7) Russell, E. V.; Israeloff, N. E. *Nature* **2000**, *408*, 695−698.

(8) Jérôme, B.; Commandeur, J. *Nature* **1997**, *386*, 589−592.

(9) Bengtzelius, U.; Götze, W.; Sjölander, A. *J. Phys. C* **1984**, *17*, 5915−5934.

(10) Götze, W.; Sjögren, L. *Transp. Theory Stat. Phys.* **1995**, *24*, 801−853.

(11) Li, G.; Du, W. M.; Chen, X. K.; Cummins, H. Z.; Tao, N. J. *Phys. Rev. A* **1992**, *45*, 3867−3879.

(12) Schönhals, A.; Kremer, F.; Hofmann, A.; Fischer, E. W.; Schlosser, E. *Phys. Rev. Lett.* **1993**, *70*, 3459−3462.

(13) Mohanty, U. *J. Chem. Phys.* **1994**, *100*, 5905−5909.

(14) Moynihan, C. T.; Shrieder, J. *J. Non-Cryst. Solids* **1993**, *160*, 52−59.

(15) Spielberg, J. I.; Gelerinter, E. *Phys. Rev. B* **1984**, *30*, 2319−2333.

(16) Ye, J. Y.; Hattori, T.; Nakatsuka, H.; Maruyama, Y.; Ishikawa, M. *Phys. Rev. B* **1997**, *56*, 5286−5296.

(17) Deschenes, L. A.; Vanden Bout, D. A. *Science* **2001**, *292*, 255−258.

(18) Deschenes, L. A.; Vanden Bout, D. A. *J. Phys. Chem. B* **2001**, *105*, 11978−11985.

(19) Biju, V.; Takeuchi, M.; Umemura, K.; Gad, M.; Ishikawa, M. *Jpn. J. Appl. Phys.* **2002**, *41*, 1579−1586.

(20) English, D. S.; Harbron, E. J.; Barbara, P. F. *J. Chem. Phys.* **2001**, *114*, 10479−10485.

(21) Lenhart, J. L.; van Zanten, J. H.; Dunkers, J. P.; Parnas, R. S. *Macromolecules* **2001**, *34*, 2225−2231.

(22) Hou, Y.; Bardo, A. M.; Martinez, C.; Higgins, D. A. *J. Phys. Chem. B* **2000**, *104*, 212−219.

(23) Keddie, J. L.; Jones, R. A. L.; Cory, R. A. *Europhys. Lett.* **1994**, *27*, 59−64.

(24) Forrest, J. A.; Dalnoki-Veress, K.; Stevens, J. R.; Dutcher, J. R. *Phys. Rev. Lett.* **1996**, *77*, 2002−2005.

(25) Biju, V.; Yamauchi, M.; Ishikawa, M. *J. Photochem. Photobiol. A. Chem.* **2001**, *140*, 237−241.

(26) Ishikawa, M.; Watanabe, M.; Hayakawa, T.; Koishi, M. *Anal. Chem.* **1995**, *67*, 511−518.

(27) Ishikawa, M.; Yogi, O.; Ye, J. Y.; Yasuda, T. *Anal. Chem.* **1998**, *70*, 5198−5208.

(28) Ye, J. Y.; Ishikawa, M.; Yogi, O.; Okada, T.; Maruyama, Y. *Chem. Phys. Lett.* **1998**, *288*, 885−889.

(29) A circularly polarized laser beam has been used as an excitation source, without the use of the standard epi-illumination scheme, as described in ref 27. The laser beam passed outside a microscope and directly irradiated a surface on which single molecules were immobilized. The angle of incidence of the laser beam was ∼60°, with respect to the surface normal. Thus, the circularly polarized beam that we used is equivalent to two circularly polarized beams that simultaneously irradiate a surface: one is along the surface normal, and the other is perpendicular to the surface normal. If the angle of incidence is 45° in this scheme, single molecules on a surface will equally be irradiated. In ref 19, we evaluated a histogram of single-molecule photocounts using excitation with ∼60° incidence, not 45°. Individual Texas Red (TR) molecules were covalently immobilized on a glass surface. The fluorescence efficiency of TR is 1.0, thus allowing the breadth of the histogram to be free from fluctuation of nonradiative relaxation. The breadth of the histogram is as narrow as that determined only by the radiation noise. This observation suggests that a difference in the incidence angle between ∼60° and 45° provides no significant contribution for the breadth of the histogram. A possible reason for insensitivity to the incidence angle may be fluctuation in the orientation of transition dipoles of individual molecules. In the current work, we used the same experimental setup that had been used in refs 19 and 27. For this reason, the effect of molecular orientations on the breadth of the histogram may not be a major factor, especially for individual Cy3 molecules that are immobilized on a glass surface without a PVAc overlayer.

(30) Pierce, R. A.; Berg, R. A. *J. Chem. Phys.* **1969**, *51*, 1267.

(31) Waldeck, D. H.; Fleming, G. R. *J. Phys. Chem.* **1981**, *85*, 2614−2617.

(32) Van der Auweraer, M.; Van den Zegel, M.; De Schryver, F. C.; Boens, N.; Willig, F. *J. Phys. Chem.* **1986**, *90*, 1169−1175.

(33) Green, M. D.; Patonay, G.; Ndou, T.; Warner, I. M. *J. Inclusion Phenom. Mol. Recognit. Chem.* **1992**, *13*, 181−193.

(34) Gruber, H. J.; Hahn, C. D.; Kada, G.; Riener, C. K.; Harms, G. S.; Ahrer, W.; Dax, T. G.; Knaus, H.-G. *Bioconjugate Chem.* **2000**, *11*, 696−704.

(35) Kohn, F.; Hofkens, J.; Gronheid, R.; Van der Auweraer, M.; De Schryver, F. C. *J. Phys. Chem. A* **2002**, *106*, 4808−4814.

(36) Luengo, G.; Ortega, F.; Rubio, R. G.; Rey, A.; Prolongo, M. G.; Masegosa, R. M. *J. Chem. Phys.* **1994**, *100*, 3258−3267.

(37) Bhattacharyya, S.; Bagchi, B. *J. Chem. Phys.* **1997**, *106*, 7262−7267.

(38) Ishikawa, M.; Ye, J. Y.; Maruyama, Y.; Nakatsuka, H. *J. Phys. Chem. A* **1999**, *103*, 4319−4331.

(39) Achibat, T.; Boukenter, A.; Duval, E.; Lorentz, G.; Etienne, S. *J. Chem. Phys.* **1991**, *95*, 2949−2954.